Advances in Bioresearch
Adv. Biores., Vol 16 (6) November 2025: 256-267
©2025 Society of Education, India
Print ISSN 0976-4585; Online ISSN 2277-1573
Journal's URL:http://www.soeagra.com/abr.html
CODEN: ABRDC3
DOI: 10.15515/abr.0976-4585.16.6.256267

Advances in Bioresearch

ORIGINAL ARTICLE

Harnessing Plant-Based Nanotechnology for Efficient Dye Degradation in Water Purification

Anuradha Ch.S.[1] and Sridevi B.[2]
[1]Department of Chemistry, Dr. V. S Krishna Government Degree & PG College (A), Visakhapatnam-530013, Andhra Pradesh, India.
[2] Department of Chemistry, Government Degree College for Women, Guntur, Andhra Pradesh, India.
Corresponding Author: Anuradha Ch.S.
Email: anuradhachippada79@gmail.com

ABSTRACT
An eco-concious and cost-efficient approach is developed to synthesize Ag-Co bimetallic nanoparticles from the extract of Abutilon indicum leaves with silver nitrate and cobalt nitrate precursor solutions. The phytochemicals in this extract serve as natural agents responsible for reduction, stabilization, and capping in biosynthesized nanoparticles. Characterization study is performed using Ultraviolet-Visible (UV-Vis) analysis, FTIR, FESEM, EDX, and HRTEM analytical techniques. These nanoparticles are served as effective photocatalyst to degrade methylene blue dye under solar irradiation. Under optimal conditions, a maximum photodegradation of 87.56% is achieved for a 10 ppm solution of the dye at pH 8 undergoes reaction with 50 mg catalyst dosage under 120 minutes of irradiation.
Keywords: *Bimetallic nanoparticles, Abutilon indicum, Methylene blue, Phytochemicals, Photodegradation.*

Received 24.09.2025 Revised 09.10.2025 Accepted 19.11.2025

How to cite this article:
Anuradha Ch.S. and Sridevi B.. Harnessing Plant-Based Nanotechnology for Efficient Dye Degradation in Water Purification. Adv. Biores. Vol 16 [6] November 2025. 256-267

INTRODUCTION

Nanotechnology is an advanced domain of science that focuses on structures ranging from 0.1 to 100 nm in size [1]. In recent times, nanotechnology and nanomaterials attract significant attention due to their vast range of applications [2]. Nanoparticles can be synthesized primarily through two approaches viz. the bottom-up technique, which involves the organization of atoms or molecules to synthesize nanoparticles and the top-down technique, which entails reducing bulk materials into increasingly smaller structures through processes like etching [3]. Nanoparticles exhibit distinctive physical properties, including a large surface area, specific shape, aggregation behavior, size distribution, surface morphology, crystallinity, solubility, and structural defects [4]. Their photocatalytic activity and stability are largely influenced by surface chemistry and zeta potential [5]. Compared to bulk materials, nanoparticles possess unique physical and chemical properties, making them highly valuable in various fields [6]. They find applications in medicine, material manufacturing, environmental science, electronics, and numerous other industries [7]. It is possible to produce copper, silver, gold platinum, palladium, iron, nickel, and cobalt nanoparticles through chemical, physical, and biological processes [8]. Nonetheless, methods of chemical synthesis often require toxic reagents which might be absorbed onto the surface of the metals and with hazardous effects [9]. Conversely, biological synthesis methods are regarded as more environmentally friendly as well as less expensive than the chemical and physical methods of producing nanoparticles [10]. Plant extract, microorganisms, fungi [11, 12], and enzymes [13, 14] are some of the sources that can be used for nanoparticle synthesis and are a step towards environmentally friendly and cost-effective methods of nanotechnology. Even so, bimetallic nanoparticles that consist of two or more single metals are far more advanced than monometallic nanoparticles in science and technology [15, 16]. For drug delivery, luminescence tagging, imaging, labeling, and biomedical research, biosynthesized bimetallic nanoparticles are finding applications due to their enhanced characteristics [17]. It is also

important to note that these unique nanoparticles have other potential uses due to their exceptional catalytic activity [18]. Environmental pollution remains one of the most critical and urgent challenges in the modern world.Textile industry releases coloured water during fabric dyeing process into the environment. Industries rigorously dealing with harmful materials such as dyestuff, distilleries, tanneries and paper mills also release highly coloured waste water into ecosystem which reasons pollution [19].

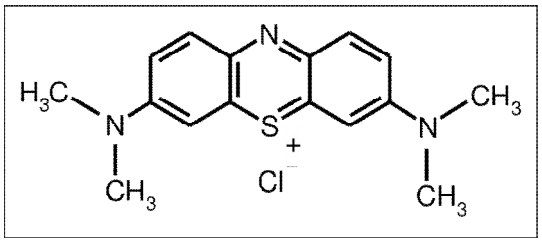

Fig. 1: Methylene blue: molecular structure

Methylene Blue (MB) is a water-soluble vibrant blue coloured crystalline dye that belongs to the cationic thiazine group [20] with chemical formula $C_{16}H_{18}ClN_3S$ (Fig. 1). It is largely used in industries including textile, pharmaceutical, medical, aquaculture, and chemical. When MB enters waterbodies, it may harm aquatic life by preventing photosynthesis and lowering oxygen levels. Methyleneblue in wastewater can have serious negative health impacts, such as respiratory discomfort, stomach issues, cyanosis, and tissue necrosis [21]. For the elimination of such harmful dyes, the photocatalytic process has been reported to be more advantageous and can degrade many organic chemicals when compared to other conventional and routine degradation strategies of dyes. *Abutilon Indicum*, a widely recognized Indian shrub from the Malvaceae family, is known as mallow in English. It has been traditionally valued in medicine for its analgesic, anti-inflammatory, anti-diabetic, laxative, emollient, and blood-tonic properties [22]. Herein, an effortless green sustainable approach has been documented for synthesizing Ag-Co bimetallic nanoparticles (BNPs) utilizing *Abutilon indicum* leaf extract as agent with reducing-cum stabilizing properties. Additionally, these BNPs serve as effective catalysts for the photodegradation of methylene blue dye when irradiated with solar light across different experimental conditions.

MATERIAL AND METHODS

MATERIALS: This research makes use of analytical-grade silver nitrate and cobalt nitrate.as chemical reagents. Deionized water is employed for cleaning glassware, preparing solutions, and conducting various experimental procedures. Fresh *Abutilon indicum* leaves are sourced from the botanical garden maintained by Dr. V.S. Krishna Government Degree and PG College (Autonomous), located in Visakhapatnam city, Andhra Pradesh state of India.

PREPARATION OF *Abutilon indicum* LEAF EXTRACT

A total of 100 grams of fresh *Abutilon indicum* Leaves are first weighed and then subjected to thorough washing under running tap water to remove all the surface impurities, subsequently treated with deionized water to wash away any traces of impurities. Following cleaning, the leaves are allowed to dry under shade for eight days. Once dried, the leaves are finely chopped and ground into a uniform powder through a household blender. This powdered sample is preserved in an airtight container and refrigerated at 4 °C. For extract preparation, 10 g of the stored leaf sample is introduced into 250 mL volume of deionized water contained in a 500 mL glass beaker. The mixture is then heated at 50 °C for 35 minutes with gentle stirring at regular intervals using a glass rod. After cooling to 25 °C , the extract is filtered twice with Whatman No.1 qualitative filter paper. This resulting filtrate, referred to as the leaf extract, is preserved at 4 °C under refrigerated conditions until further application.

Fig. 2.1. ***Abutilon indicum*** **plant**

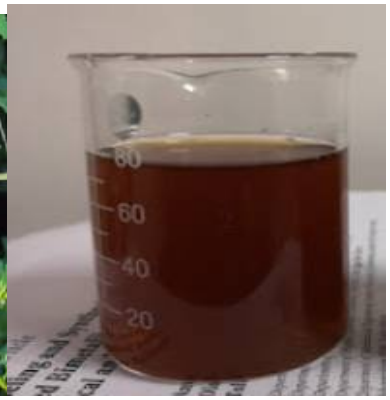

Fig. 2.2. Abutilon indicum leaf extract

SYNTHESIS OF AG-CO BIMETALLIC NANOPARTICLES

To prepare silver-cobalt (Ag-Co) bimetallic nanoparticles (BNPs), equimolar (25 mM) aqueous solutions of silver nitrate ($AgNO_3$) and cobalt nitrate ($Co(NO_3)_2$) are separately prepared. Specifically, 0.4246 g of $AgNO_3$ and 0.7275 g of $Co(NO_3)_2$ are individually dissolved in 100 mL deionized water in different volumetric flasks. For the nanoparticle synthesis, 100 mL of the prepared silver nitrate solution is transferred into a 500 mL beaker, and 90 mL of *Abutilon indicum* leaf extract is gradually introduced using a burette. Following this, 100 mL of cobalt nitrate solution is also administered dropwise into the reaction system. Now,the beaker is continuously stirred using a magnetic stirrer to ensure uniform mixing throughout the process. The reaction is maintained at 50°C for 45 minutes under constant stirring at pH 7.

When the reaction has proceeded to completion, these synthesized bimetallic nanoparticles are collected through centrifugation at 4500 rpm for 30 minutes. To remove any residual impurities, the obtained nanoparticles are washed twice with deionized water. The purified Ag-Co BNPs are then collected and stored for further characterization.

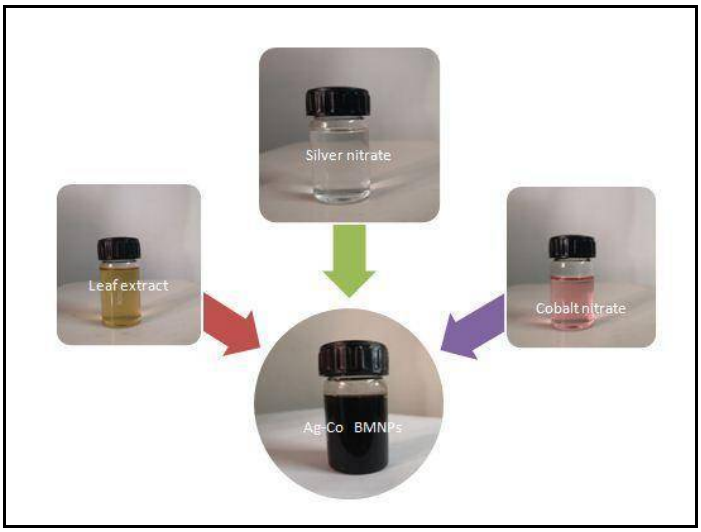

Fig. 2.3: **Schematic Representation of Ag-Co BNPs Synthesis**

CHARACTERIZATION OF NANOPARTICLES:

The successful formation of Ag-Co BNPs is verified through multiple analytical techniques. UV-Visible absorption spectroscopy is performed using a UV-2450 SHIMADZU double-beam spectrophotometer to confirm optical properties. Functional group determination is conducted via Infrared spectroscopic characterization using FTIR with Bruker instrument. Morphological and elemental characterization using SEM and EDX with a Hitachi S-3700N system. Additionally, the structural and morphological characteristics of the BNPs are obtained by advanced structural analysis using HRTEM with an FEI Technai instrument.

RESULTS AND DISCUSSION

ULTRAVIOLET-VISIBLE (UV-VIS) SPECTRAL ANALYSIS:

The absorption spectrum in the UV–Visible region for Ag-Co BNPs is depicted in Fig. 3.1. A distinct peak of plasmonic resonance at the nanoparticle surface is observed at approximately 442 nm, which serves as an indication of the nanoscale nature of the synthesized particles. This characteristic absorption band confirms the successful formation of Ag-Co BNPs [23].

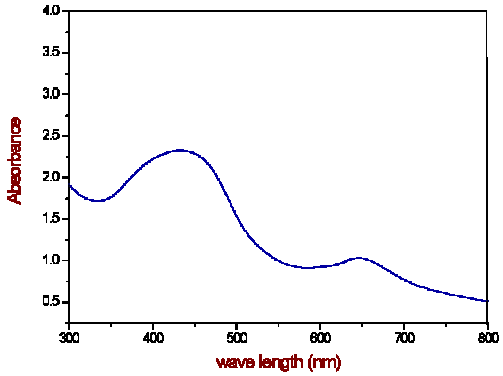

Fig. 3.1. UV-Visible Spectrum of leaf extract

FTIR SPECTRAL ANALYSIS:

FTIR spectroscopy is employed to identify the characteristic functional groups in the biomolecules of the *Abutilon indicum* leaf extract, which offer the crucial contribution to the bioreduction of Ag^{+} and Co^{2+} ions, as well as facilitating the capping and structural stabilization of Ag-Co BNPs. The recorded FTIR spectra display prominent peaks, which are analyzed by comparing against standard reference values to determine the specific functional groups associated with both the leaf extract and the formed Ag-Co BNPs. The FTIR spectra of *Abutilon indicum* leaf extract and Ag-Co BNPs synthesized using the extract are illustrated in Fig. 3.2(a) and Fig. 3.2(b), respectively. A comparative analysis of these spectra reveals the presence of various phytochemicals, including polyphenols, terpenes, carbohydrates, amides, and amines, on the surface of Ag-Co BNPs [24]. These biomolecules contribute to the reduction process and provide stability to the nanoparticles.

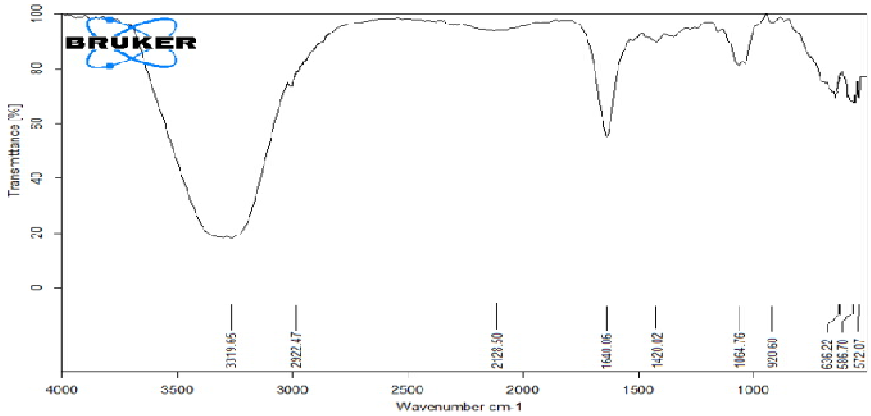

Fig. 3.2 (a). FTIR analysis of extract of *Abutilon indicum* leaves

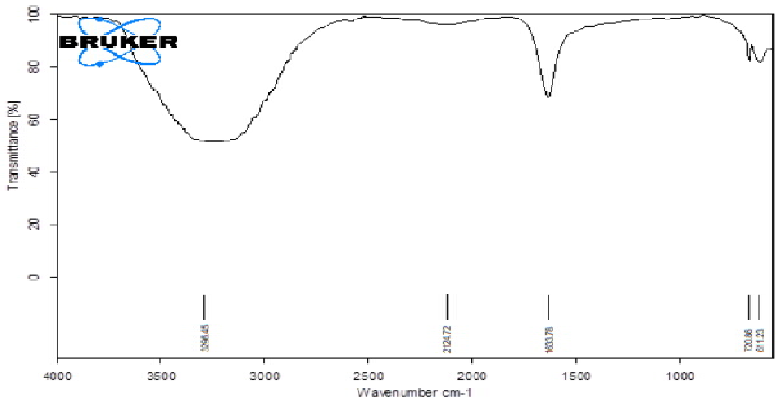

Fig. 3.2 (b). FTIR spectral analysis of Ag-Co BNPs

Characterization by FTIR technique provides crucial analytical tool utilized to determine the presence of functional groups involved in reducing metal precursor ions and the stabilization of obtained nanoparticles. In this study, FTIR analysis is conducted to detect the occurrence of biomolecular constituents in both *Abutilon indicum* leaf extract and the bio-synthesized Ag-Co BNPs. The FTIR results for the leaf extract and synthesized nanoparticles are depicted in Fig. 3.2(a) and Fig. 3.2(b), respectively. Key absorption peaks were observed at 3319, 2922, 1640, 1420, 1064, and 700–500 cm^{-1}. A prominent and broad absorption band at 3319 cm^{-1} is assigned to O–H bond stretching, typically associated with phenols or carboxylic acid groups in the extract. The additional peaks at 2922, 1640, 1420, 1064, and 700–500 cm^{-1} correspond to stretching vibrations of C–H and C=O groups, along with aromatic C–H bending frequencies, C-O-C bond stretching, and C-Cl vibrations, respectively. The FTIR analysis reveals that most of the absorption bands observed in the *Abutilon indicum* leaf extract are also present in the synthesized Ag-Co bimetallic nanoparticles (BNPs), either at the same positions or with slight shifts. The key bands detected in the nanoparticles appear at 3296, 2124, 1633, 720, and 611 cm^{-1}. The sustained appearance of these absorption features in the Ag-Co BNPs suggests that the nanoparticle surfaces are coated with various plant-derived secondary metabolites, including glycosides, amino acids, carbohydrates, saponins, phytosterols, flavonoids, phenolic compounds, tannins, proteins, and diterpenes. These metabolites contain functional groups such as phenols, carboxylic acids, amides, ketones, aldehydes, and alkyl halides, which contribute to the stability of the BNPs. The analysis provides additional evidence for the presence of carbonyl and hydroxyl functional groups in the leaf extract, which are Suggested to be a key factor in the bio-reduction of Ag^{+} and Co^{2+} ions, facilitating nanoparticle synthesis. Additionally, the coating of plant biomolecules on the nanoparticle surfaces contributes to their enhanced stability, preventing agglomeration and supporting the formation of a well-dispersed bimetallic alloy structure.

SEM IMAGING AND EDX SPECTRAL ANALYSIS:

Energy Dispersive X-ray (EDX) spectroscopy was utilized to determine the Elemental profile of the synthesized Ag-Co BNPs using *Abutilon indicum* leaf extract. The EDX spectrum, presented in Fig. 3.3(a), along with the elemental composition data in Table 1, confirms the presence of silver (Ag) and cobalt (Co), verifying the successful formation of Ag-Co BNPs. Additionally, the EDX analysis provides quantitative information regarding the proportions of silver and cobalt within the synthesized BNPs. Scanning Electron Microscopy (SEM) is utilized to examine the morphological characteristics of the Ag-Co BNPs at different magnifications, as depicted in Fig. 3.3(b). The obtained SEM micrographs reveal that the BNPs exhibit a well-defined structure with diameters ranging between 30 and 100 nm. These findings further validate the formation of bimetallic nanoparticles with nanoscale dimensions, supporting their potential applications in various fields.

Table: 1. Quantitative assessment of the BNPs

Element	Atomic percentage
Cobalt	38.46
Silver	61.54
totals	100.0

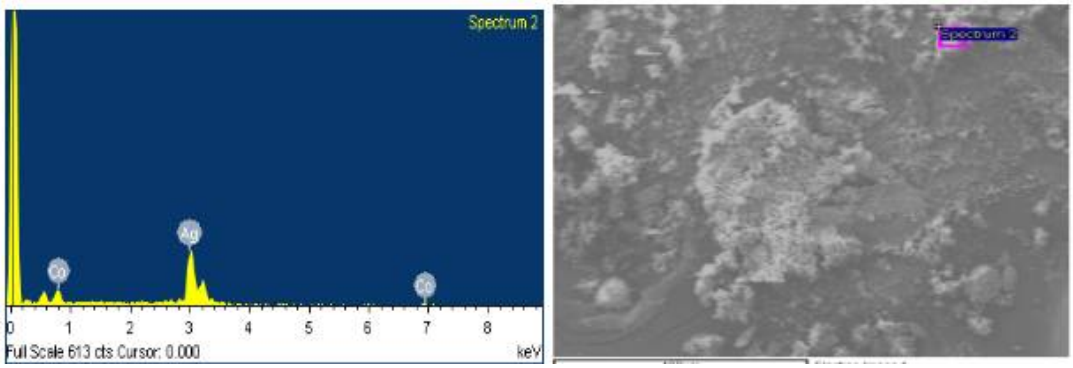

Fig. 3.3 (a). EDX Analysis of Ag-Co BNPs

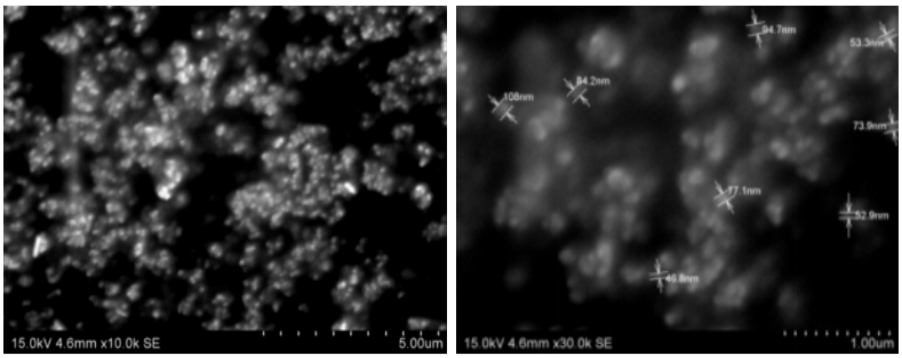

Fig. 3.3 (b). Morphological Characterization of Ag-Co BNPs Using SEM

HIGH-RESOLUTION TRANSMISSION ELECTRON MICROSCOPY (HRTEM) CHARACTERIZATION*:*
Fig 3.4 displays the HRTEM images of Ag-Co BNPs synthesized using *Abutilon indicum* leaf extract. The images reveal that the Ag-Co BNPs predominantly exhibit a spherical morphology and possess a well-defined crystalline structure with dimensions below 100 nm. Notably, the images depict two metal nanoparticles positioned in close proximity, forming a bilobal-like configuration. These findings are further corroborated by the SEM analysis, confirming the structural characteristics of the fabricated BNPs.

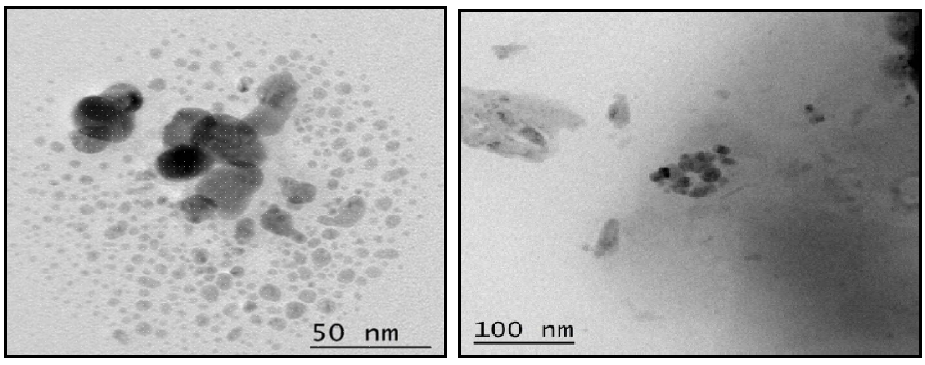

Fig. 3.4. HRTEM images of Ag-Co BNPs

PHOTOCATALYTIC TREATMENT OF METHYLENE BLUE CONTAMINANT USING AG-CO BNPS:
The photocatalytic degradation of Methylene Blue (MB) dye is studied using green-synthesized Ag-Co BNPs as the catalyst. A stock solution of 50 ppm methylene blue dye solution is initially prepared. Reaction mixtures are formulated by adding varying amounts of Ag-Co BNPs (series of weights: 10, 20, 30, 40, 50, 60, 70, and 80 mg) into 100 mL of MB dye solution at different concentrations (tested concentrations included 5, 10, 15, 20, 25, and 30 ppm). The pH of the solutions is adjusted (ranging from pH 3 to 10) through the controlled addition of 0.1 N sulfuric acid or sodium hydroxide as required.
Before exposure to sunlight, the reaction mixture is subjected to stirring in a dark environment for 20 minutes to achieve an adsorption-desorption equilibrium between the MB dye molecules and Ag-Co

BNPs. The photocatalytic process takes place under natural sunlight irradiation between 10:30 AM and 3:30 PM. At regular intervals of 30 minutes, samples are withdrawn, centrifuged to isolate solid catalyst particles, and analyzed using a UV-Visible spectrophotometer to examine their optical absorption properties. The degradation efficiency is evaluated by monitoring changes in absorbance under different conditions, such as reaction time, pH variation, dye concentration, and catalyst dosage. The characteristic absorbance peak of MB dye is recorded at 668 nm [25]. The percentage degradation of the MB dye solution is determined based on the equation given below.

$$\% \text{ degradation} = \left(\frac{A_0 - A_t}{A_0}\right) \times 100 \quad \ldots \quad (1)$$

Where, A_0 represents the initial absorbance of the MB solution, while At denotes the absorbance of the solution after degradation at a specific time t (in minutes) [26].

The proposed mechanism for the photocatalytic degradation process is outlined below.

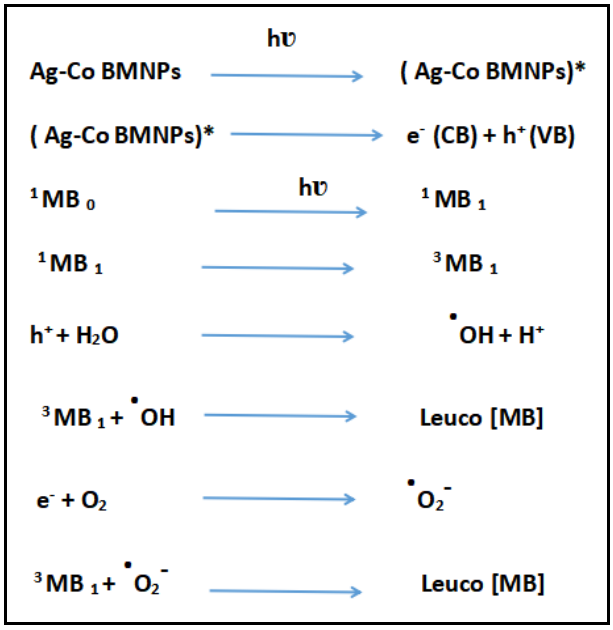

Upon absorbing radiation of a suitable wavelength, The MB dye transitions to its first excited singlet state triggered by the absorption of photons. Through inter-system crossing (ISC), it further shifts to the triplet state. Simultaneously, Ag-Co BNPs absorb the incident radiation, exciting an electron from the valence band to the conduction band. The hole formed in the valence band interacts with H_2O, leading to the production of hydroxyl radicals (•OH) and protons (H^+). The ·OH radicals oxidize MB dye into its leuco form, which subsequently breaks down into a colorless product. Meanwhile, the excited electron is captured by molecular oxygen, forming superoxide anion radicals ($\cdot O_2^-$). These anion radicals transform the MB dye into its leuco form, and further degrades into products.

IMPACT OF CONTACT DURATION:

The photodegradation efficiency of Ag-Co BNPs on MB dye is evaluated through batch-mode experiments. The degradation performance is anticipated to improve with raising levels of contact time. To study this effect, a 100 mL solution of MB dye (10 ppm) is treated with 10 mg of Ag-Co BNPs as a catalyst at pH 7. The results, depicted in Fig. 4(a) and Fig. 4(b), illustrate the influence of contact time on the degradation process. Initially, the degradation of dye using BNPs occurs rapidly, but as the contact time increases, after 90 minutes, the degradation rate gradually slows down and eventually reaching a nearly constant percentage [27]. This phenomenon occurs due to the intense adsorption interactions between the dye molecules and Ag-Co BNPs, as well as the availability of numerous catalytically active sites available in the early phase of the reaction. However, after approximately 100 minutes, the percentage of degradation gradually stabilizes, approaching a nearly constant value. This behavior is associated with the depletion of vacant reactive centers on the catalyst surface limiting further adsorption of dye molecules and leading to equilibrium in the degradation process [28, 29].

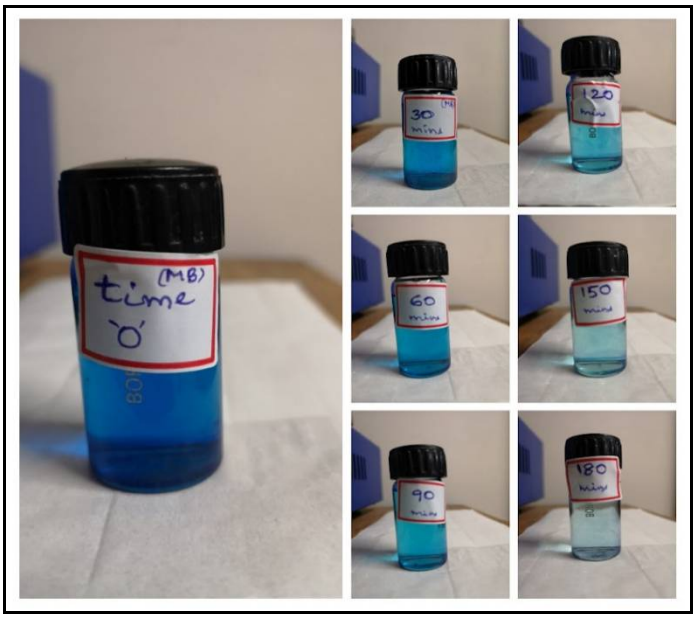

Fig. 4(a). Colour change in MB dye at various time intervals

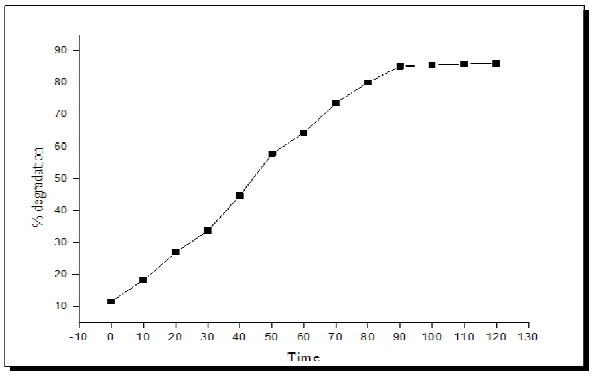

Fig. 4(b):Impact of Contact Time on Photodegradation

ROLE OF INITIAL DYE CONCENTRATION ON PHOTODEGRADATION

The initial concentration of solution of MB dye influences the photodegradation rate. To assess this effect, the BNPs catalyst dosage is maintained at 10 mg, and the pH is set to 7, and the irradiation time is fixed at 180 minutes. To investigate concentration-dependent degradation, the initial MB dye levels are set at 5, 10, 15, 20, and 25 ppm. The photodegradation rate is graphically represented in Fig. 4(c). As illustrated in the figure, it is evident that maximum degradation efficiency is observed at 5 ppm, followed by a gradual decline as the dye concentration increases [30, 31]. This trend can be owing to, at lower initial higher abundance of dye molecules readily adsorb onto the BNPs' surface, leading to efficient degradation. However, as the dye concentration increases beyond 5 ppm, the solution becomes more intensely colored, preventing sufficient photon penetration and thereby reducing the degradation efficiency there by only fewer photons can reach the BNPs surface. Therefore, the % photodegradation is reduced when concentration of dye is high [32]. Thus in the present case 5-10 ppm dye solutions can be considered optimum concentration to produce efficient photodegradation upto 85-78% on a 10 mg nanocatalyst under the sunlight.

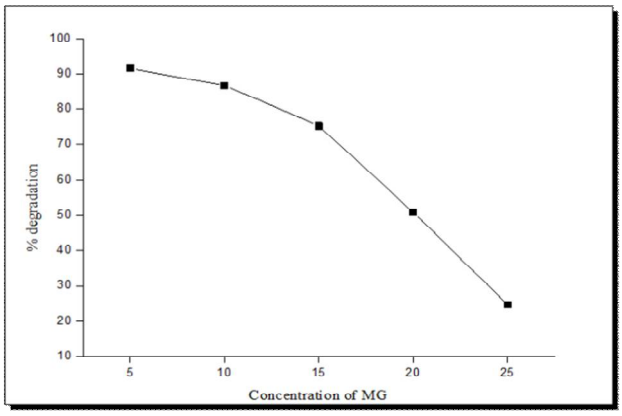

Fig. 4(c): Impact of MB Dye Concentration on Photodegradation Efficiency

INFLUENCE OF PH ON PHOTODEGRADATION

The pH of the dye solution is instrumental in determining the adsorption behavior of the dye on the photocatalyst. In this study, the initial concentration of the dye solution is maintained at 10 ppm, while the photocatalyst dosage is kept constant at 10 mg, with an irradiation time of 120 minutes. The effect of pH is analyzed by preparing solutions with pH conditions spanning from 3 to 10. The corresponding degradation efficiencies are evaluated and presented in Fig. 4(d).

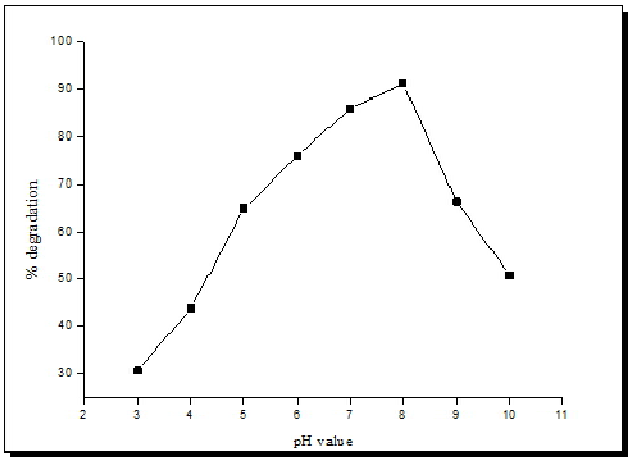

Fig. 4(d): Influence of pH on Efficiency of Photodegradation

It has been noted that elevation in the pH of the MB dye solution enhances its degradation on the photocatalyst, reaching an optimal rate at pH 8. This initial increase in photodegradation efficacy is primarily because of the greater availability of OH^- ions at higher pH levels. These hydroxyl ions interact with the positive holes (h^+) in the semiconductor, generating hydroxyl radicals (•OH), which significantly contribute to the degradation process. However, beyond pH 8, the degradation rate declines. This reduction may be due to the MB dye losing its cationic nature in the presence of excessive OH^- ions, leading to electrostatic repulsive interactions between the dye molecules and the anionic semiconductor surface. Consequently, this repulsion hinders the photocatalytic degradation process [33, 34]. Based on these observations, pH 8 was identified as the optimal pH for efficient photodegradation.

EFFECT OF VARYING CATALYST DOSAGE ON PHOTODEGRADATION

In the photodegradation process, The amount of photocatalyst significantly influences the decolorization of the dye solution. Optimizing the catalyst dosage is essential to maximize photon absorption while minimizing the wastage of costly catalysts [35]. To determine the optimal dosage, experiments are conducted by varying amounts of catalyst (10–80 mg) are added to 100 mL of 10 ppm MB dye solution maintained at pH 7, with a reaction time of 90 minutes. The degradation efficiency of MB under these conditions is illustrated in Fig. 4(e).

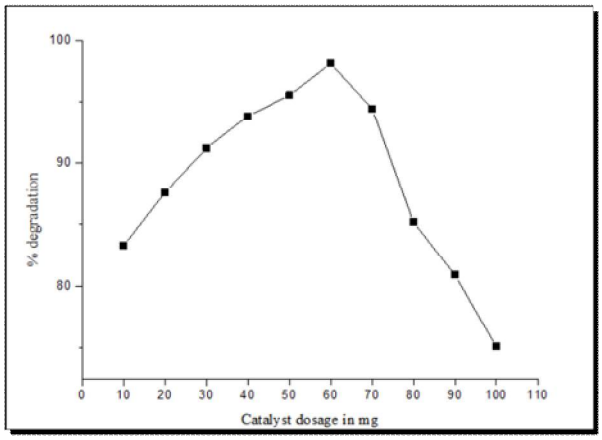

Fig. 4(e): Influence of Catalyst Dosage on Photodegradation Efficiency

The results indicate that as the catalyst dosage increases from 10 mg to 100 mg in 100 mL of MB dye solution, the degradation efficiency improves. This enhancement occurs because a higher catalyst amount, up to 60 mg, provides more reactive sites, leading to the generation of additional reactive species. However, beyond this dosage, The diminished degradation performance arises from the formation of turbid suspensions at higher catalyst concentrations. These suspensions hinder solar light penetration into the reaction mixture, reducing the overall photocatalytic efficiency [36]. Based on these observations, 50 mg of catalyst is identified as the optimal dosage for effective MB dye degradation.

CONCLUSION

An environmentally friendly method is proposed for synthesizing Ag-Co bimetallic nanoparticles using *Abutilon indicum* leaf extract. UV-Visible spectroscopy confirms that the particles have been at the nanoscale, as indicated by the observed positions of SPR absorption bands. FTIR analysis verifies the occurrence of secondary plant metabolites from phytomolecules, which act as biological reducing and stabilizing agents for the nanoparticles. EDX, SEM, and HRTEM analyses reveal that the Ag-Co BNPs exhibit predominantly spherical-shaped structure with sizes ranging from 30 to 100 nm. The photocatalytic property of these phyto-fabricated nanoparticles is evaluated under sunlight for the degradation of MB dye, a polluting agent in the environment. The percentage of MB dye photodegradation varies with respect to factors such as contact time,dye concentration, pH, and dosage of photocatalyst . The findings of this study suggest that the optimal conditions for MB dye degradation are determined as pH 8, a catalyst weight of 50 mg, the concentration of dye with 10 ppm, and a contact time of 120 minutes, achieving a degradation efficiency of 87.56% under these conditions.

ACKNOWLEDGEMENT

The authors express their gratitude to the Department of Chemistry, Dr. V.S. Krishna Government Degree & PG College (Autonomous), for providing essential laboratory facilities for conducting the research work.

CONFLICT OF INTEREST

The authors declare that there is no conflict of interest.

REFERENCES

1. Nasrollahzadeh, M., Sajadi, S.M., Sajjadi, M., Issaabadi, Z. (2019). An introduction to nanotechnology. Interface Sci. Technol., 28:1–27.
2. Malik, S., Muhammad, K., Waheed, Y. (2023). Nanotechnology: a revolution in modern industry. Molecules, 28(2):661.
3. Abid, N., Khan, A.M., Shujait, S., Chaudhary, K., Ikram, M., Imran, M., Maqbool, M. (2022). Synthesis of nanomaterials using various top-down and bottom-up approaches, influencing factors, advantages, and disadvantages: A review. Adv. Colloid Interface Sci., 300:102597.
4. Mourdikoudis, S., Pallares, R.M., Thanh, N.T. (2018). Characterization techniques for nanoparticles: comparison and complementarity upon studying nanoparticle properties. Nanoscale, 10(27):12871–12934.
5. Phan, H.T., Haes, A.J. (2019). What does nanoparticle stability mean? J. Phys. Chem. C, 123(27):16495–16507.
6. Asha, A.B., Narain, R. (2020). Nanomaterials properties. In: Polymer Sci. Nanotechnol., pp. 343–359.

7. Kefeni, K.K., Msagati, T.A., Mamba, B.B. (2017). Ferrite nanoparticles: synthesis, characterization and applications in electronic devices. Mater. Sci. Eng. B, 215:37–55.
8. Ijaz, I., Gilani, E., Nazir, A., Bukhari, A. (2020). Detail review on chemical, physical and green synthesis, classification, characterizations and applications of nanoparticles. Green Chem. Lett. Rev., 13(3):223–245.
9. Soltys, L., Olkhovyy, O., Tatarchuk, T., Naushad, M. (2021). Green synthesis of metal and metal oxide nanoparticles: Principles of green chemistry and raw materials. Magnetochemistry, 7(11):145.
10. Bhardwaj, B., Singh, P., Kumar, A., Kumar, S., Budhwar, V. (2020). Eco-friendly greener synthesis of nanoparticles. Adv. Pharm. Bull., 10(4):566.
11. Jadoun, S., Arif, R., Jangid, N.K., Meena, R.K. (2021). Green synthesis of nanoparticles using plant extracts: A review. Environ. Chem. Lett., 19(1):355–374.
12. Fang, X., Wang, Y., Wang, Z., Jiang, Z., Dong, M. (2019). Microorganism-assisted synthesized nanoparticles for catalytic applications. Energies, 12(1):190.
13. Khan, A.U., Malik, N., Khan, M., Cho, M.H., Khan, M.M. (2018). Fungi-assisted silver nanoparticle synthesis and their applications. Bioprocess Biosyst. Eng., 41:1–20.
14. Ovais, M., Khalil, A.T., Ayaz, M., Ahmad, I., Nethi, S.K., Mukherjee, S. (2018). Biosynthesis of metal nanoparticles via microbial enzymes: A mechanistic approach. Int. J. Mol. Sci., 19(12):4100.
15. Sharma, G., Kumar, A., Sharma, S., Naushad, M., Dwivedi, R.P., ALOthman, Z.A., Mola, G.T. (2019). Novel development of nanoparticles to bimetallic nanoparticles and their composites: A review. J. King Saud Univ. Sci., 31(2):257–269.
16. Mazhar, T., Shrivastava, V., Tomar, R.S. (2017). Green synthesis of bimetallic nanoparticles and its applications: A review. J. Pharm. Sci. Res., 9(2):102.
17. Shkryl, Y., Rusapetova, T., Yugay, Y., Egorova, A., Silant'ev, V., Grigorchuk, V., Bulgakov, V. (2021). Biosynthesis and cytotoxic properties of Ag, Au, and bimetallic nanoparticles synthesized using Lithospermum erythrorhizon callus culture extract. Int. J. Mol. Sci., 22(17):9305.
18. Tiri, R.N.E., Gulbagca, F., Aygun, A., Cherif, A., Sen, F. (2022). Biosynthesis of Ag–Pt bimetallic nanoparticles using propolis extract: Antibacterial effects and catalytic activity on NaBH4 hydrolysis. Environ. Res., 206:112622.
19. Islam, T., Repon, M.R., Islam, T., Sarwar, Z., Rahman, M.M. (2023). Impact of textile dyes on health and ecosystem: A review of structure, causes, and potential solutions. Environ. Sci. Pollut. Res., 30(4):9207–9242.
20. Yang, Y., Zhu, Q., Peng, X., Sun, J., Li, C., Zhang, X., Zhang, Y. (2022). Hydrogels for the removal of the methylene blue dye from wastewater: A review. Environ. Chem. Lett., 20(4):2665–2685.
21. Oladoye, P.O., Ajiboye, T.O., Omotola, E.O., Oyewola, O.J. (2022). Methylene blue dye: Toxicity and potential elimination technology from wastewater. Results Eng., 16:100678.
22. Srivastava, S.P., Dikshit, S., Moharana, A., Chaturvedi, N., Sharma, S., Verma, P. (2024). Abutilon indicum: Bioactive Compounds and Diverse Therapeutic Applications. Curr. Nutraceuticals, 5(1):e170124225755.
23. Xing, Y., Bai, X.H., Zhang, Y., Hu, G.M., Gao, L.G., Qi, P.C., Bai, M.M. (2023). Facile synthesis of Ag-Co bimetallic nanoparticles decorated Fe3O4@EDTA nanocomposites and their enhanced catalytic activity. J. Magn. Magn. Mater., 579:170857.
24. Rafique, M., Tahir, R., Gillani, S.S.A., Tahir, M.B., Shakil, M., Iqbal, T., Abdellahi, M.O. (2022). Plant-mediated green synthesis of zinc oxide nanoparticles from Syzygium cumini for seed germination and wastewater purification. Int. J. Environ. Anal. Chem., 102(1):23–38.
25. Upadhyay, L.S.B., Tirkey, A., Bhagat, P., Singh, S.K., Mishra, A. (2025). Green Synthesis of Copper Oxide Nanoparticles Using Solanum tuberosum Extract to Mediate Photocatalytic Degradation of Methylene Blue. Plasmonics, 1–16.
26. Rafiq, S., Raza, Z.A., Aslam, M., Bakhtiyar, M.J. (2022). Graphene nanosheets decorated with copper oxide nanoparticles for the photodegradation of methylene blue. Chem. Res. Chin. Univ., 38(6):1518–1525.
27. Bhat, S.A., Zafar, F., Mondal, A.H., Kareem, A., Mirza, A.U., Khan, S., Nishat, N. (2020). Photocatalytic degradation of carcinogenic Congo red dye in aqueous solution, antioxidant activity, and bactericidal effect of NiO nanoparticles. J. Iran. Chem. Soc., 17:215–227.
28. Fouda, A., Hassan, S.E.D., Saied, E., Hamza, M.F. (2021). Photocatalytic degradation of real textile and tannery effluent using biosynthesized magnesium oxide nanoparticles (MgO-NPs), heavy metal adsorption, phytotoxicity, and antimicrobial activity. J. Environ. Chem. Eng., 9(4):105346.
29. Munagapati, V.S., Wen, H.Y., Gollakota, A.R., Wen, J.C., Shu, C.M., Lin, K.Y.A., Zyryanov, G.V. (2022). Magnetic Fe3O4 nanoparticles loaded papaya (Carica papaya L.) seed powder as an effective and recyclable adsorbent material for the separation of anionic azo dye (Congo Red) from liquid phase: Evaluation of adsorption properties. J. Mol. Liq., 345:118255.
30. Senthil Kumar, P., Sivaranjanee, R., Vinothini, U., Raghavi, M., Rajasekar, K., Ramakrishnan, K. (2013). Adsorption of dye onto raw and surface modified tamarind seeds: isotherms, process design, kinetics and mechanism. Desalin. Water Treat., 52(13–15):2620–2633.
31. Ahmed, M.A., Abou-Gamra, Z.M., Medien, H.A.A., Hamza, M.A. (2017). Effect of porphyrin on photocatalytic activity of TiO2 nanoparticles toward Rhodamine B photodegradation. J. Photochem. Photobiol. B, 176:25–35.
32. Mohamed, R.M., McKinney, D., Kadi, M.W., Mkhalid, I.A., Sigmund, W. (2016). Platinum/zinc oxide nanoparticles: enhanced photocatalysts degrade malachite green dye under visible light conditions. Ceram. Int., 42(8):9375–9381.

33. Isai, K.A., Shrivastava, V.S. (2017). Photocatalytic degradation of methylene blue using ZnO and 2% Fe–ZnO nanocomposites. J. Mater. Sci. Mater. Electron., 28(12):8760–8770.
34. Mishra, V., Sharma, A., Ojha, H., Mishra, R.K., Dubey, R., Sharma, P.K. (2021). A review on green synthesis and applications of iron-based nanomaterials. Mater. Today Chem., 19:100399.
35. Bhatti, M.S., Areeb, A., Kumar, S., Kumar, V., Sharma, S., Naushad, M., Iqbal, J. (2021). Efficient removal of toxic Congo red dye using activated carbon prepared from waste biomass. J. Mol. Liq., 334:116022.
36. Singh, V.K., Kumar, R., Singh, P., Saxena, A., Hasan, S.H. (2020). A review on the synthesis and applications of nanomaterials for the remediation of pollutants from wastewater. Environ. Nanotechnol. Monit. Manag., 14:100333.